ACS Catalysis

Research Article

pubs.acs.org/acscatalysis

Acid Strength Controlled Reaction Pathways for the Catalytic Cracking of 1-Pentene to Propene over ZSM-5

Long F. Lin, Shu F. Zhao, Da W. Zhang, Hui Fan, Yue M. Liu,* and Ming Y. He

Shanghai Key Laboratory of Green Chemistry and Chemical Processes, Department of Chemistry, East China Normal University, North Zhongshan Road 3663, Shanghai 200062, People's Republic of China

Supporting Information

ABSTRACT: The influence of acid strength was evaluated toward the selectivity to propene on conversion of 1-pentene. For the catalytic cracking of 1-pentene, the main reaction pathways and the molar ratio of propene to ethene (P/E ratio) were controlled by acid strength with the appropriate amount of total acid sites. The results showed that the P/E ratio increased with decreasing amounts of strong acid sites, since the activation energies of individual reaction pathways were influenced by acid strength to a different extent. Strong acid sites could promote pathway I′ ($C_5^{2-} \rightarrow C_2^{2-} + C_3^{2-}$) and pathway II′-1 ($C_6^{2-} \rightarrow C_2^{2-} + C_4^{2-}$), while weak acid sites preferred pathway II′ ($2C_5^{2-} \rightarrow C_{10}^{+} \rightarrow C_4^{2-} + C_6^{2-}$) and pathway II′-2 ($C_6^{2-} \rightarrow 2C_3^{2-}$), since pathways II′ and II′-2 underwent some energetically favorable routes (tertiary−secondary, secondary−secondary) of carbenium ion intermediates. By manipulation of the acid strength distribution on ZSM-5, the P/E ratio and selectivity of propene could be significantly improved, suggesting that this can provide an important guideline for improving such a process. In addition, we also designed a coupled process combing butene and pentene coconversion, as pentene and butene could be produced during C_4^{2-} and C_5^{2-} catalytic cracking. The coupled process could offer a promising solution to gain high selectivity of propene from C_4 and C_5 olefin cracking.

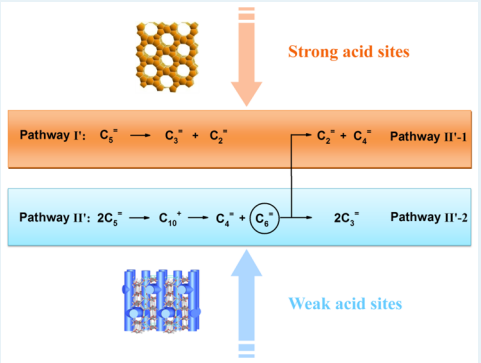

KEYWORDS: *1-pentene catalytic cracking, ZSM-5, reaction pathways, acid strength, propene*

1. INTRODUCTION

Propene is one of the most indispensable petrochemicals.[1] Due to the rapidly growing demand for propene, the catalytic cracking of low-value C_4 and C_5 olefins to propene has drawn much interest.[2−9] In addition, as the fluid catalytic cracking (FCC)[10] and methanol-to-olefin (MTO) processes[11] produce numerous low-value C_4 and C_5 olefins, the catalytic valorization of these olefins is invariably anticipated. As this cracking reaction contains various side reactions, such as dehydrogenation−aromatization,[12−15] hydrogen transfer reactions,[12,13,16] dealkylation,[6,12,13] and coke formation,[17−20] the introductions of phosphorus,[21−26] alkali-metal ions,[4,27−29] and alkaline-earth metals[30] were adopted to modify the acidity of zeolites and then to suppress side reactions. Recently, we have systematically investigated the catalytic cracking of 1-butene to propene over ZSM-5[31] and also found that the selectivity of propene could be improved by reducing the acid strength of the zeolite. It should be noted that around 21% pentene is a byproduct with propene in the catalytic cracking of 1-butene.[31] Thus, an investigation of the catalytic cracking of 1-pentene rather than 1-butene is more significant. The side reactions of 1-pentene catalytic cracking are similar to those of 1-butene catalytic cracking,[31,32] but still there are some essential differences. The monomolecular cracking of butene is energetically highly unfavorable,[33] but a competition between monomolecular and dimerization−cracking pathways exists in the catalytic cracking of 1-pentene. In comparison with the catalytic cracking of 1-butene, more insights need to be gained into the different and more complex reaction pathways of the catalytic cracking of 1-pentene.

In the monomolecular cracking pathway, 1-pentene undergoes protonation and isomerization to form 2-pentyl carbenium ions and/or 3-methyl-1-pentyl carbenium ions. Then β-scission produces ethene and propene (Scheme 1).[7−9] Apart from this, the cracking of pentene can proceed through oligomeric carbenium ion intermediates (C_{10}^{+}).[9] Miyaji and co-workers[7] have investigated the dimerization−cracking mechanism for the conversion of pentene over SAPO-5 at the initial stage. First, 2,3,4,5-tetramethyl-2-hexyl carbenium ion (X) and 3,4,5-trimethyl-3-heptyl carbenium ion (Y) are produced by the dimerization of pentenes. The experimental results showed that butenes were the main product, indicating that the β-scission of decyl carbenium ions favored the production of butenes and hexenes. After isomerization and cracking of decyl carbenium ions, the generated hexenes continued to crack to propene or ethene and butene.[34] On the basis of previous studies, a plausible reaction network of pentene conversion is shown in Scheme 1. The main reactions include two pathways: pathway

Received: September 15, 2014
Revised: May 22, 2015
Published: May 26, 2015

DOI: 10.1021/cs501967r
ACS Catal. 2015, 5, 4048−4059

Scheme 1. Possible Main and Side Reactions Network for 1-Pentene Cracking over ZSM-5[a]

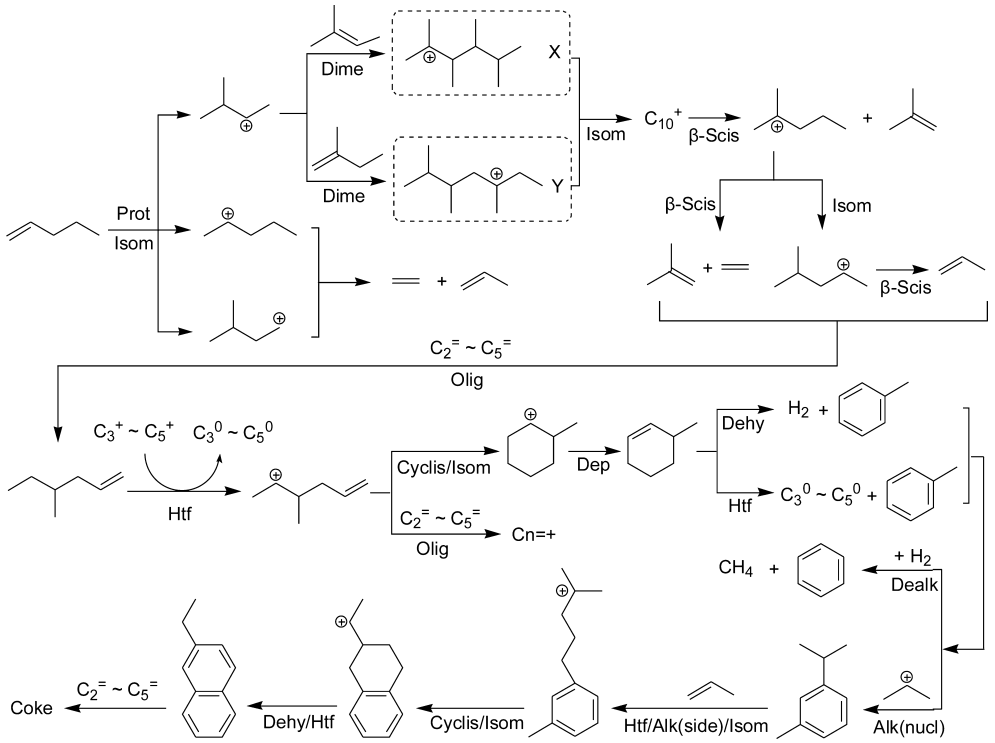

[a]Abbreviations: Prot, protonation; Dep, deprotonation; Dime, dimerization; *β*-Scis, *β*-scission; Htf, hydrogen transfer; Mtf, methyl transfer; Isom, isomerization; Olig, oligomerization; Dehy, dehydrogenation; Cyclis, cyclization; Alk(side), alkylation side chain; Alk(nucl), alkylation aromatic nucleus.

Scheme 2. Reaction Pathways of Monomolecular Cracking and Dimerization−Cracking of 1-Pentene

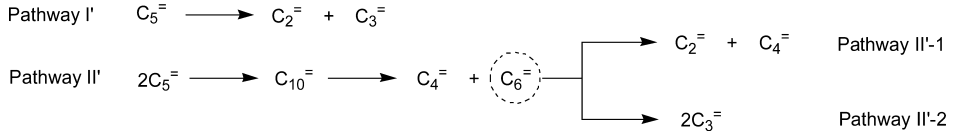

I′ ($C_5^{2-} \rightarrow C_2^{2-} + C_3^{2-}$) and pathway II′ ($2C_5^{2-} \rightarrow C_{10}^+ \rightarrow C_4^{2-} + C_6^{2-}$). As C_6^{2-} could continue to crack, pathway II′ has two subsequent branches: pathway II′-1 ($C_6^{2-} \rightarrow C_2^{2-} + C_4^{2-}$) and pathway II′-2 ($C_6^{2-} \rightarrow 2C_3^{2-}$).[34−36] The side reactions of dehydrogenation−aromatization[12−15] and hydrogen transfer[12,13,16] mostly produce aromatics, alkanes, and hydrogen. In principle, side reactions should be suppressed, and then the main pathway II′ and pathway II′-2 should be strengthened to improve the selectivity of propene and of propene/ethene ratio (P/E ratio).

Miyaji et al.[7] found that a spatial volume of zeolite that was almost the same as the volume of pentyl cations promoted the monomolecular cracking of pentene, while a larger zeolite cavity favored the dimerization−cracking reaction pathway. With ferrierite, the P/E mole ratio was around 1, because monomolecular cracking of pentene was dominant. However, ZSM-5 gave a P/E mole ratio of approximately 1.8, due to the formation of the decyl carbenium ions.[7] Bortnovsky et al.[9] achieved similar results by investigating the cracking of 2-methyl-2-butene using various zeolite and zeotype catalysts. To the best of our knowledge, there is no report on how to control the main reaction pathways of catalytic cracking of pentenes via modifying the acid strength of zeolites, which is one of the key factors of acid zeolites for improvement of the P/E ratio.

According to the main reaction pathways summed up in Scheme 2, some essential theoretical estimation could be made on the basis of the carbon balance. For example, if half of the pentenes underwent monomolecular cracking (i.e., pathway I′) with C_2^{2-} and C_3^{2-} as the products, then the others would undergo pathway II′, producing C_4^{2-} and C_6^{2-}. In addition, if the intermediate C_6^{2-} were further transformed through pathways II′-1 and II′-2 also in equal proportions, then the P/E ratio would be 1.2 while the P/B ratio (propene/butene ratio) would be 2. However, in actual reactions, it is difficult to directly figure out the proportion each pathway accounts for. Therefore, we supposed pathway II′ accounts for a, while pathway I′ accounts for $1 - a$. Meanwhile, for the conversion of intermediate C_6^{2-}, II′-2 was assumed to account for b and II′-1 for $1 - b$. Then on the basis of the carbon balance, we could improve the P/E ratio by controlling the acid strength of zeolite according to a and b, as $P/E = (1 - a + ab)/(1 - 0.5a - 0.5ab)$, while $P/B = (1 - a + ab)/(a - 0.5ab)$. Hence, in this paper, we attempt to control the main reaction pathways to improve the P/E ratio by means of designing acid strength on ZSM-5, which has been reported to be inverse proportion to the reaction activation energy.

DOI: 10.1021/cs501967r
ACS Catal. 2015, 5, 4048−4059

2. EXPERIMENTAL SECTION

2.1. Catalyst Preparation. A series of ZSM-5 zeolites with different Si/Al_2 mole ratios were prepared by hydrothermal synthesis and are denoted as ZSM-5(n), n representing the Si/Al_2 mole ratio detected by ICP. Typically, aluminum isopropoxide (24.7 wt % Al_2O_3, Sinopharm Chemical Reagent Co., Ltd.) was first dissolved in deionized water, into which was then added tetrapropylammonium hydroxide (TPAOH, 25 wt %, Sinopec Co., Ltd.) as the structure-directing agent. After the mixture was stirred at room temperature for 2 h, tetraethyl orthosilicate (28.4 wt % SiO_2, Sinopharm Chemical Reagent Co., Ltd.) was added, and then the mixture was stirred for another 2 h, resulting in a gel with a chemical composition of 1 SiO_2:x Al_2O_3:0.25 TPAOH:15 H_2O (x was determined by the desired Si/Al_2 mole ratio). The gel was transferred into a 100 mL Teflon-lined stainless steel autoclave which was heated statically at 170 °C for 48 h. The solid products were filtered, washed with deionized water, dried overnight at 80 °C, and finally calcined at 550 °C in air for 6 h.

ZSM-5 zeolites with different acid strength distributions were designed and denoted Z-1−Z-5, respectively. Z-1 was prepared by impregnating 10 g of ZSM-5(43) into 10 mL of phosphoric acid aqueous solution containing 1.9 wt % phosphorus, followed by drying at 50 °C for 24 h under vacuum and 120 °C for 4 h and finally calcination at 550 °C for 6 h.[21,37] Z-2 with 1.6 wt % phosphorus was obtained from ZSM-5(55) using the same method as for Z-1. ZSM-5(86) was leached with 6 mol L^{-1} HNO_3 at reflux for 5 h with continuous stirring, followed by washing with water, drying, and then calcination at 550 °C for 6 h.[38] After all these procedures, Z-3 was successfully obtained. Z-5 was achieved from ZSM-5(61) with the same method, but a relatively lower acid concentration (2 mol L^{-1} HNO_3) was employed to treat the ZSM-5(61). Z-4 was obtained directly from ZSM-5(142) without any treatment.

2.2. Catalyst Characterization. The catalysts were characterized by various techniques, including XRD, SEM, BET, ICP, NH_3-TPD, and ^{27}Al and ^{31}P solid-state MAS NMR.[31] Thermogravimetric (TG) analyses were carried out on a Mettler Toledo TGA/SDTA851^e instrument with a ramping rate of 10 K min^{-1} in an air flow of 40 mL min^{-1}. The Brönsted and Lewis acid sites of the samples were investigated by FT-IR of adsorbed pyridine in an in situ cell with CaF_2 windows. Wafers with a weight of 25 mg and radius of 6.5 mm were degassed for 1 h under vacuum at 600 °C. Then pyridine was admitted, and after equilibration, the samples were outgassed for 0.5 h at increasing temperatures (150, 200, 250, 350, and 450 °C). The spectra were recorded on a Nicolet iS50 FT-IR spectrometer.

2.3. Catalytic Testing. Catalytic cracking of 1-pentene over the zeolites were carried out in a stainless steel continuous-flow reactor (10 mm i.d.), with a thermocouple in the center of the catalyst bed. The catalyst was pressed, crushed, and sorted into grains of 40−60 mesh and then was activated at 550 °C for 3 h under a nitrogen flow before each reaction run. Then 1-pentene (98%) in diluted nitrogen (N_2/1-C_5H_{10} = 9.83, mole ratio, analyzed by GC) was passed through the reactor at the desired temperature. The output products were analyzed online by an Agilent 7890A gas chromatograph equipped with a Agilent 19095P-M25 column (50 m × 530 μm × 15 μm), a Dikma 2 m × 1/8 5A column, a Dikma 2 m × 1/8 in. Porapak Q column, two Dikma 1 m × 1/8 in. Porapak Q columns, and an FID detector which was used to detect hydrocarbons and two TCD detectors which were used to detect hydrogen and nitrogen. For simplicity, we grouped all types of pentenes as the overall feedstock. The composition of products analyzed here by GC are mole results (the composition of calibration gas used to standardize GC is mole percent); the total amount is not constant before and after reactions, but nitrogen does not always change; thus, we use nitrogen as a reference to calculate pentene conversion. Then, the mole conversions of pentenes (equal to mass conversions), the mole selectivities of the products, the mass selectivities of products, and the mass yields of products were calculated by eqs 1−4.

$$\begin{aligned}\text{conversion} &= \frac{(n_{C_5H_{10}})_0 - (n_{C_5H_{10}})_t}{(n_{C_5H_{10}})_0} \times 100\% \\ &= \frac{(n_{N_2})_0 \times 1/9.83 - (n_{N_2})_t \times (C_5H_{10}\%)_t/(N_2\%)_t}{(n_{N_2})_0 \times 1/9.83} \\ &\quad \times 100\% \\ &= 100\% - 9.83 \times \frac{(C_5H_{10}\%)_t}{(N_2\%)_t} \times 100\% \\ (n_{N_2})_0 &= (n_{N_2})_t \end{aligned} \tag{1}$$

$$\text{mole selectivity } (C_xH_y) = \frac{(C_xH_y\%)_t}{\sum (C_iH_j\%)_t} \times 100\% \tag{2}$$

$$\begin{aligned}\text{mass selectivity } (C_xH_y) &= \frac{W(C_xH_y)_t}{\sum (W(C_iH_j)_t)} \\ &= \frac{M(C_xH_y) \times (n_{N_2})_t \times (C_xH_y\%)_t/(N_2\%)_t}{(n_{N_2})_t \times \sum (M(C_iH_j) \times (C_iH_j\%)_t/(N_2\%)_t)} \times 100\% \\ &= \frac{M(C_xH_y) \times (C_xH_y\%)_t}{\sum (M(C_iH_j) \times (C_iH_j\%)_t)} \end{aligned} \tag{3}$$

$$\text{mass yield} = \text{conversion} \times \text{selectivity} \tag{4}$$

When we verified the law of conservation of mass, nitrogen was also used as a reference. The carbon atom of input (mol h^{-1}), carbon atom of output (mol h^{-1}), mass of input (g h^{-1}), and mass of output (g h^{-1}) were calculated by eqs 5−8. Details of the calculations are given in a discussion of the conservation of mass and carbon atoms and Tables S1 and S2 in the Supporting Information.

$$\text{input carbon atom} = \frac{1}{9.83} \times (n_{N_2})_0 \times 5 \tag{5}$$

$$\text{input total mass} = \frac{1}{9.83} \times (n_{N_2})_0 \times 70 \tag{6}$$

$$\text{output carbon atom} = \sum_x \left(\frac{(C_xH_y\%)_t}{(N_2\%)_t} \times (n_{N_2})_t \times x \right) \tag{7}$$

DOI: 10.1021/cs501967r
ACS Catal. 2015, 5, 4048−4059

$$\text{output total mass} = \sum_x \left(\frac{(C_xH_y\%)_t}{(N_2\%)_t} \times (n_{N_2})_t \times M(C_xH_y) \right) \quad (8)$$

Here $(n_{C_5H_{10}})_0$, $(n_{C_5H_{10}})_t$, $(n_{N_2})_0$, and $(n_{N_2})_t$ represent the mole flows of pentenes in the feed, of pentenes in the output, of nitrogen in the feed, and of nitrogen in the output, respectively. $W(C_xH_y)_t$ (x = 0, 1, 2, 3, 5, 6, 7, 8) and $W(C_iH_j)_t$ (i = 0, 1, 2, 3, 5, 6, 7, 8) represent the mass flows of a certain product in the output and any product in the output, respectively. $(C_5H_{10}\%)_t$, $(N_2\%)_t$, $(C_xH_y\%)_t$, and $(C_iH_j\%)_t$ represent the mole compositions analyzed by GC of pentenes in the output, of nitrogen in the output, of a certain product in the output, and any product in the output, respectively. $M(C_xH_y)$ and $M(C_iH_j)$ represent the molecular weights of a certain product and any product, respectively.

3. RESULTS AND DISCUSSION

3.1. Preparation and Characterization of Z-1−Z-5. In order to investigate the influence of acid strength on the main reaction pathways, a series of ZSM-5 zeolites with different acid strengths were needed. However, as ZSM-5 had a complex crystal structure with 12 different T sites[39] in which the aluminums had various proton energies corresponding to different acid strengths,[40,41] a distribution of the acid strength on ZSM-5 instead of a single value is exhibited and could be characterized by NH_3-TPD. A typical NH_3-TPD spectrum of ZSM-5 was obtained with two maximum peaks at low and high temperatures, corresponding to the weak and strong acid sites of ZSM-5, respectively.[42] Therefore, from the NH_3-TPD result, we can easily get the ratio between the amounts of strong acid sites and weak acid sites (HC/LC ratio), which represents the relative acid strength. Through phosphoric acid and nitric acid modification, five ZSM-5 samples (Z-1−Z-5) were prepared. As shown in Table 1, from Z-1 to Z-5, the HC/LC ratios increased gradually from 0.244 to 2.627, and the amount of total acid sites of each sample is around 0.19 mmol g^{-1}.

Table 1. Acid Properties of Z-1−Z-5 Samples Measured by NH_3-TPD

zeolite	LC[a] (mmol g^{-1})	HC[b] (mmol g^{-1})	total acid sites (mmol g^{-1})	HC/LC
Z-1	0.160	0.039	0.199	0.244
Z-2	0.131	0.074	0.205	0.565
Z-3	0.076	0.115	0.191	1.513
Z-4	0.058	0.123	0.181	2.121
Z-5	0.051	0.134	0.185	2.627

[a]Low-temperature center, attributed to weak acid sites. [b]High-temperature center, attributed to strong acid sites.

It was generally believed that B acid sites played a key role in the cracking of olefins.[43] FT-IR spectroscopy with pyridine as a probe molecule was used to characterize B acid sites. Generally, the vibration band at around 1540 cm^{-1} was assigned to pyridine adsorbed on the Brönsted (B) acid sites and the band around 1450 cm^{-1} to the Lewis (L) acid sites,[44] which represent the relative amounts of B and L acid sites, respectively. The pyridine-adsorbed samples were degassed at 150 and 350 °C, respectively. The adsorption amount of pyridine degassed at a low temperature of 150 °C, corresponding to the total acid amount, whereas the adsorption amount of pyridine, degassed at relatively high temperature of 350 °C, corresponded with the acid amount of strong acid.[37] As shown in Table 2, the total amounts of B acid sites of these five

Table 2. Brönsted Acid Properties[a] of Z-1−Z-5

zeolite	weak (au)	strong (au)	total (au)	strong/weak
Z-1	0.056	0.008	0.064	0.14
Z-2	0.047	0.011	0.058	0.23
Z-3	0.033	0.035	0.068	1.06
Z-4	0.030	0.034	0.064	1.13
Z-5	0.026	0.040	0.066	1.54

[a]Detected by FT-IR spectroscopy after adsorption of pyridine.

samples were similar and the strong/weak acid ratios also increased from Z-1 to Z-5. In addition, a semiquantitative study of the strength of B acid sites was also carried out using FT-IR spectroscopy with adsorbed pyridine. To evaluate this parameter, we defined the ratio as the normalized area at temperature T, which is between the Brönsted absorption band area measured after pyridine adsorption followed by evacuation at temperature T and at 150 °C. This quantity, calculated for B acid site absorption bands, has been plotted as a function of evacuation temperature in Figure 1. The more quickly the

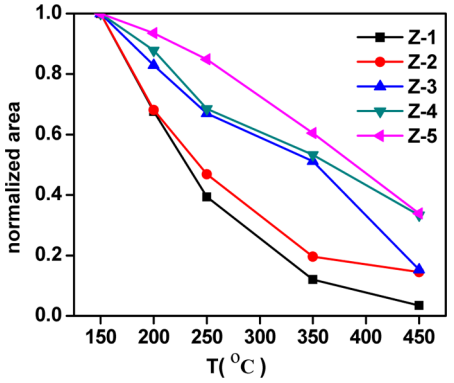

Figure 1. Normalized area relative to Brönsted acid sites versus evacuation temperature.

normalized area decreased, the weaker the acid strength.[45] As can be seen from Figure 1, the strength of B acid sites over Z-1 was the weakest, and from Z-1 to Z-5, the strength gradually increased. Obviously, the results of FT-IR spectroscopy after adsorption of pyridine fit well with the results of NH_3-TPD.

The approaches of modification by phosphoric acid and nitric acid were employed to obtain Z-1−Z-5 (except Z-4, see the section 2.1), so that their acid strengths were greatly different. NH_3-TPD was used to characterize the acidities of ZSM-5 modified by phosphoric acid, which showed that after treatment the total amount of acid sites decreased and the number of strong acid sites decreased noticeably while the number of weak acid sites did not decrease as much.[21,25,31] In addition, the acidities of these samples were measured using FT-IR spectroscopy with pyridine as the probe molecule. As shown in Table 3, the amount of B acid sites decreased after phosphoric acid treatment. More specifically, the number of weak B acid sites remained almost the same while the number of strong B acid sites decreased dramatically. On investigation of the L acid sites, a similar phenomenon appeared. Therefore,

DOI: 10.1021/cs501967r
ACS Catal. 2015, 5, 4048−4059

Table 3. Acidity Properties[a] of ZSM-5 and Modified ZSM-5

	Brönsted acid (~1540 cm^{-1})				Lewis acid (~1450 cm^{-1})				Brönsted and Lewis acid			
zeolite[b]	weak (au)	strong (au)	total (au)	strong/weak	weak (au)	strong (au)	total (au)	strong/weak	weak (au)	strong (au)	total (au)	strong/weak
ZSM-5(55)	0.059	0.094	0.153	1.59	0.025	0.030	0.055	1.20	0.084	0.124	0.208	1.48
ZSM-5(55)-1.6P	0.047	0.011	0.058	0.23	0.019	0.008	0.027	0.42	0.066	0.019	0.085	0.29
ZSM-5(86)	0.050	0.049	0.099	0.98	0.055	0.061	0.116	1.11	0.105	0.110	0.215	1.05
ZSM-5(86)-D6	0.033	0.035	0.068	1.06	0.017	0.018	0.035	1.06	0.050	0.053	0.103	1.06
ZSM-5(61)	0.061	0.036	0.097	0.59	0.081	0.073	0.154	0.90	0.142	0.109	0.251	0.77
ZSM-5(61)-D2	0.026	0.040	0.066	1.54	0.012	0.016	0.028	1.33	0.038	0.056	0.094	1.47

[a]Detected by FT-IR spectroscopy after adsorption of pyridine. [b]Legend: ZSM-5(55)-1.6P, modified by phosphoric acid and containing 1.6 wt % phosphorus, also denoted Z-2; ZSM-5(86)-D6, dealumination from ZSM-5(86) using 6 mol L^{-1} HNO_3, also denoted Z-3; ZSM-5(61)-D2, dealumination from ZSM-5(61) using 2 mol L^{-1} HNO_3, also denoted Z-5.

Table 4. Catalytic Cracking of 1-Pentene at Different Temperatures over ZSM-5(142)[a]

			sel (mol %)											
T (°C)	conv(C_5^{2-}) (mol %)	TOF (h^{-1})	C_2^{2-}	C_3^{2-}	C_4^{2-}	C_6^{2-}	$C_1^0 + C_2^0$	C_3^0–C_5^0	H_2	arom	P/E (mol)	P/B (mol)	a	b
450	93.6	567.1	19.3	36.1	20.7	4.9	0.5	13.5	1.6	3.5	1.9	1.7	0.688	0.688
475	94.6	573.1	23.7	34.2	16.9	3.2	1.0	14.6	2.5	4.0	1.5	2.0	0.563	0.623
500	96.3	583.4	28.2	35.5	14.9	4.3	1.1	9.2	2.8	4.0	1.3	2.4	0.467	0.569
525	97.5	590.8	35.2	36.3	12.8	1.3	1.5	5.1	3.4	4.5	1.0	2.8	0.342	0.379
550	98.5	596.8	41.3	36.5	10.6	0.7	1.7	3.8	3.4	2.0	0.9	3.4	0.229	0.027

[a]Reaction conditions: cat., ZSM-5(142), 1.0 g; pressure, 0.1 MPa; 1-pentene flow rate, 0.2 mL min^{-1}; N_2 flow rate, 320 mL min^{-1}; WHSV, 7.68 h^{-1}; TOS, 0.5 h.

the total number of weak acid sites decreased slightly but that of strong acid sites experienced a remarkable decline, which was consistent with the results of NH_3-TPD.

In comparison with the phosphoric acid modification, the phenomenon of nitric acid treatment was rather different. After treatment with 6 mol L^{-1} HNO_3, the amounts of B acid and L acid of ZSM-5(86) both decreased. With regard to acid strength, it was interesting to note that regardless of B acid or L acid, the numbers of strong acid sites and weak acid sites decreased at the same step, resulting in almost no change in the strong/weak acid ratio (Table 3). Previous NH_3-TPD results also showed that the HC/LC ratio remained almost unchanged (ZSM-5(86), 1.697; ZSM-5(86)-D6, 1.513).[31] After leaching by 2 mol L^{-1} HNO_3, an obvious decline in the number of weak B acid sites in ZSM-5(61) was seen, whereas the number of strong B acid sites remained stable. However, the numbers of weak and strong L acid sites decreased to a similar extent. Then, the strong/weak acid ratio of total B and L acid sites experienced some rise from 0.77 to 1.47 (Table 3). Similarly, an increase from 2.096 to 2.627 of the HC/LC ratio gained from NH_3-TPD was also observed.[31] In conclusion, nitric acid treatment favored the removal of weak acid sites or the removal of weak and strong acid sites at a similar step, which depended on the concentration of HNO_3 and the parent zeolites, whereas phosphoric acid modification favored a decrease in the number of strong acid sites. Thus, using different parent zeolites and employing different treatment methods, a series of zeolties (Z-1–Z-5) with various acid strengths but similar numbers of acid sites was successfully achieved. However, the XRD patterns, ^{27}Al MAS NMR spectra, SEM, and BET showed that the other physicochemical properties of Z-1–Z-5 were approximately identical.[31]

3.2. Influence of Temperature. Bortnovsky et al.[9] investigated the cracking of 2-methyl-2-butene by using various zeolite and zeotype catalysts, including ZSM-5, ZSM-11, ZSM-12, SAPO-11, ferrierite, mordenite, and beta. Only ZSM-5 and ZSM-11 zeolites exhibited a high and stable selectivity to C_2–C_4 olefins with a high conversion level. In this paper, we chose ZSM-5 zeolite for the catalytic cracking of 1-pentene. In the catalytic cracking of 1-butene, the side reactions could be suppressed by decreasing the number of total acid sites of zeolites. When ZSM-5(142) was chosen as the catalyst, the number of total acid sites of which was 0.181 mmol g^{-1} and the byproducts were suppressed to around 20%.[31] Here, the influence of temperature on catalytic cracking of 1-pentene was studied over ZSM-5(142).

Table 4 shows the reaction results of catalytic cracking of 1-pentene at different temperatures over ZSM-5(142). When the reaction temperature was increased, the conversion of pentenes experienced a slight growth, as did the TOF. The total selectivity of byproducts was not more than 22.0%, which meant that the side reactions in the catalytic cracking of 1-pentene were also suppressed over ZSM-5(142). The selectivity of ethene showed a stable increase from 19.3% to 41.3% when the reaction temperature was raised from 450 to 550 °C, while the selectivity of butene decreased from 20.7% to 10.6% and the selectivity of propene remained stable at 36%. It was interesting to note that, at 500 °C, P/E = 1.3 and P/B = 2.4. In theory, if 50% of C_5^{2-} underwent pathway II′ (a = 0.5) and 50% of C_6^{2-} underwent pathway II′-2 (b = 0.5), it would lead to P/E = 1.2, and P/B = 2. In this experiment, a = 0.467 and b = 0.569 were calculated from P/E = 1.3 and P/B = 2.4, which are close to the theoretical values of a and b. Although the experimental results are highly consistent with the theoretical analysis, the difference in P/B ratios between the experimental value (P/B = 2.4) and the theoretical value (P/B = 2) cannot be ignored. In theoretical analysis, we assumed that all the C_4^{2-} produced during the cracking reaction were remained unchanged, but in fact, a small part of C_4^{2-} might take part in the following reactions. This is why the experimental value of the P/B ratio is slightly higher than the theoretical value. When the reaction temperature was decreased to below 500 °C, it

DOI: 10.1021/cs501967r
ACS Catal. 2015, 5, 4048–4059

Table 5. Catalytic Cracking of 1-Pentene over Z-1−Z-5 at 450 °C[a]

			sel (mol %)											
zeolite	conv(C_5^{2-}) (mol %)	TOF (h^{-1})	C_2^{2-}	C_3^{2-}	C_4^{2-}	C_6^{2-}	$C_1^0 + C_2^0$	C_3^0−C_5^0	H_2	arom	P/E (mol)	P/B (mol)	*a*	*b*
Z-1	84.5	465.9	12.0	41.9	31.6	5.7	0.1	6.7	0.4	1.7	3.5	1.3	0.904	0.731
Z-2	86.7	464.1	13.7	40.7	28.9	5.6	0.2	8.8	0.5	1.6	3.0	1.4	0.858	0.730
Z-3	93.5	537.1	19.0	37.2	21.9	4.9	0.4	13.1	1.1	2.5	2.0	1.7	0.706	0.694
Z-4	93.6	567.1	19.3	36.1	20.7	4.9	0.5	13.5	1.6	3.5	1.9	1.7	0.688	0.688
Z-5	94.1	557.6	20.5	31.3	17.5	4.3	0.7	18.5	2.1	5.0	1.5	1.8	0.618	0.618

[a]Reaction conditions: cat., 1.0 g; temperature, 450 °C; pressure, 0.1 MPa; 1-pentene flow rate, 0.2 mL min^{-1}; N_2 flow rate, 320 mL min^{-1}; WHSV, 7.68 h^{-1}; TOS, 0.5 h.

Table 6. Output Distribution in Catalytic Cracking of Different Feedstocks over Z-1

		output distribn (wt %)									
entry	feedstock	C_2^{2-}	C_3^{2-}	C_4^{2-}	C_5^{2-}	C_6^{2-}	$C_1^0 + C_2^0$	C_3^0−C_5^0	H_2	arom	P/E (wt)
1[a]	butene	4.8	30.3	44.3	11.8	4.3	0.1	3.6	0	0.9	6.3
2[b]	pentene	14.8	33.5	26.4	14.8	4.0	0.1	4.6	0	1.8	2.3
4[c]	butene + pentene	7.9	27.4	39.6	17.8	2.9	0.1	3.1	0	1.2	3.5

[a]Reaction conditions: cat., Z-1, 1.0 g; temperature, 500 °C; pressure, 0.1 MPa; 1-butene flow rate, 40 mL min^{-1}; N_2 flow rate, 320 mL min^{-1}; TOS, 1.5 h. [b]Reaction conditions: cat., Z-1, 1.0 g; temperature, 500 °C; pressure, 0.1 MPa; 1-pentene flow rate, 0.2 mL min^{-1}; N_2 flow rate, 320 mL min^{-1}; TOS, 0.5 h. [c]Reaction conditions: cat., Z-1, 1.0 g; temperature, 500 °C; pressure, 0.1 MPa; 1-butene flow rate, 20 mL min^{-1}; 1-pentene flow rate, 0.1 mL min^{-1}; N_2 flow rate, 320 mL min^{-1}; mole ratio of 1-butene and 1-pentene, 1:1; TOS, 0.5 h.

gave rise to P/E > 1.3, and P/B < 2.4. In contrast, P/E < 1.3 and , P/B > 2.4 were found when the reaction temperature was raised to beyond 500 °C. In addition, the values of *a* and *b* declined when the reaction temperature was increased. As pathway I′ ($C_5^{2-} \leftrightarrow C_2^{2-} + C_3^{2-}$) is a reversible reaction, raising the reaction temperature would benefit both the forward reaction rate and reverse reaction rate, but with the forward reaction rate being changed more. Pathway II′ ($2C_5^{2-} \leftrightarrow C_{10}^{+} \rightarrow C_4^{2-} + C_6^{2-}$) is also a reversible reaction, but its reverse reaction rate could be increased more than the forward reaction rate when the temperature was raised. Therefore, raising the temperature could promote pathway I′ while suppressing pathway II′: i.e., the *a* value could be decreased. In conclusion, the reaction temperature has a significant influence on the reaction pathway: low temperature is beneficial to promote pathways II′ and II′-2. Thus, the P/E ratio could be improved by a reduction in the reaction temperature.

3.3. Influence of Acid Strength. In section 3.2, the values of *a* and *b* were improved to 0.688 through a decrease in the reaction temperature to 450 °C. In this section, we will investigate the influence of acid strength on the main reaction pathways in detail and find out whether it is possible to further improve the values of *a* and *b* by adjusting the acid strength.

As shown in Table 5, catalytic cracking of 1-pentene over Z-1−Z-5 at 450 °C was performed. With an increase in the acid strength distribution, the conversion of pentenes increased, and the TOF also showed an upward trend. A rise in the selectivity of ethene was observed from 12.0% to 20.5%, while the selectivity of propene and butenes decreased from 41.9% to 31.3% and from 31.6% to 17.5%, respectively. The P/E ratio dipped to only 1.5 from 3.5 when the HC/LC ratio was improved from 0.244 (Z-1) to 2.627 (Z-5); meanwhile, the P/B ratio experienced a slight growth from 1.3 to 1.8. According to P/E ratios and P/B ratios, *a* and *b* values were determined and are given in Table 5. It is interesting to note that the *a* and *b* values showed a downward trend with an increase in acid strength.

It is known that reaction activation energies can be strongly reduced if the acid strength is increased, and notably, the rates for different reaction pathways were also increased to a different extent.[46] In this case, how does the acid strength influence the main reactions of the catalytic cracking of pentenes? As the main reaction network was complicated and the activation energy of each step was difficult to evaluate by experiments, we summed them up to investigate the apparent activation energy. The steps for cracking of C_5^{2-} molecules to C_2^{2-} and C_3^{2-} are classified as pathway I′, and the apparent activation energy of pathway I′ is denoted $E_{I'}$. Similarly, pathway II′ includes the dimerization steps of C_5^{2-} molecules to C_{10}^{+} and then cracking to C_4^{2-} and C_6^{2-}. Pathway II′-1 contains the steps for cracking of C_6^{2-} molecules to C_2^{2-} and C_4^{2-}, and pathway II′-2 contains the steps for cracking of C_6^{2-} molecules to C_3^{2-}. The apparent activation energies of pathways II′, II′-1, and II′-2 are denoted as $E_{II'}$, $E_{II'-1}$, and $E_{II'-2}$, respectively.

Then there are two possible situations concerning the effect of acid strength on activation energies of pathways I′ and II′. If the acid strength displayed greater effect on $E_{I'}$ than on $E_{II'}$, increasing acid strength would result in a faster decrease of $E_{I'}$ in comparison to that of $E_{II'}$. As we know, the reaction rate is indicated by the reaction rate constant (k). Thus, as $E_{I'}$ decreased more quickly than $E_{II'}$, the reaction rate constant of pathway I′ ($k_{I'}$) would increase more quickly than that of pathway II′ ($k_{II'}$) according to the Arrhenius equation ($k = Ae^{-E_a/RT}$),[47] meaning that the improvement in the reaction rate of pathway I′ is faster than that of pathway II′. Thus, improving acid strength could promote pathway I′ while decreasing the *a* value. In contrast, if the acid strength displayed a smaller effect on the activation energy of pathway I′ in comparison to that of pathway II′, the *a* value would be improved by an increase in acid strength. Obviously, the experimental result that the *a* value decreased with an increase in acid strength of ZSM-5 suggests that the first situation is reasonable. Therefore, pathway II′ could be promoted by decreasing the number of strong acid sites over ZSM-5.

For the relationship between pathways II′-1 and II′-2, there are also two possible effects of acid strength on the apparent activation energies, which could lead to opposite results. If the effect of acid strength on the activation energy of pathway II′-1

DOI: 10.1021/cs501967r
ACS Catal. 2015, 5, 4048−4059

Table 7. Output Mass and Conversion in Catalytic Cracking of Different Feedstocks over Z-1

			output mass (g)										
entry	feedstock	input mass (g)	C_2^{2-}	C_3^{2-}	C_4^{2-}	C_5^{2-}	C_6^{2-}	$C_1^0 + C_2^0$	C_3^0–C_5^0	H_2	arom	conv(C_4^{2-}) (wt %)	conv(C_5^{2-}) (wt %)
1[a]	butene	56	2.7	17.0	24.8	6.6	2.4	0	2.0	0	0.5	55.7	
2[b]	pentene	70	10.4	23.4	18.5	10.4	2.8	0.1	3.2	0	1.3		85.2
3[c]	butene + pentene	126	13.0	40.4	43.3	17.0	5.2	0.1	5.2	0	1.8	22.7	75.8
4[d]	butene + pentene	126	9.9	34.6	49.9	22.5	3.6	0.1	3.9	0	1.6	11.1	67.9

[a]Reaction conditions: the same as those in Table 6, entry 1; total input, 56 g of 1-butene. [b]Reaction conditions: the same as those in Table 6, entry 2; total input, 70 g of 1-pentene. [c]Hypothetical conditions: entries 1 and 2 in one reactor, but with no interplays between their reactions. [d]Reaction conditions: the same as those in Table 6, entry 4; total input, 56 g of 1-butene and 70 g of 1-pentene.

Table 8. Production Selectivity in Catalytic Cracking of Mixed Feedstocks over Z-1

		sel (wt %)							
entry	feedstock	C_2^{2-}	C_3^{2-}	C_6^{2-}	$C^0 + C_2^0$	C_3^0–C_5^0	H_2	arom	P/E (wt)
3[a]	butene + pentene	19.8	61.5	7.9	0.2	8.0	0	2.7	3.1
4[b]	butene + pentene	18.4	64.3	6.8	0.2	7.3	0	2.9	3.5

[a]Conditions: the same as those in Table 7, entry 3. [b]Conditions: the same as those in Table 7, entry 4.

was greater than that of pathway II′-2, increasing acid strength would give rise to a faster decrease of $E_{II'-1}$ in comparison to that of $E_{II'-2}$, which means that strong acid sites preferred pathway II′-1. Therefore, the *b* value would decrease with increasing acid strength. In contrast, if the acid strength displayed a smaller effect on the activation energy of pathway II′-1 in comparison to that of pathway II′-2, the results would be opposite. However, the experimental result that the *b* value decreased with an increase in acid strength of ZSM-5 was consistent with the first situation. Thus, weak acid sites preferred pathway II′-2. In conclusion, when there is a decrease in the number of strong acid sites of ZSM-5, the P/E ratio can be improved because of the promotion of pathways II′ and II′-2. On Z-1 with the lowest number of strong acid sites, *a* and *b* values soared to 0.904 and 0.731, respectively, giving rise to a value of 3.5 for the P/E ratio (Table 5).

3.4. Influence of Cofeed. Experimental results have showed that a considerable amount of pentenes remained[31] in the system of 1-butene conversion over Z-1, while numerous butenes were produced in the conversion of 1-pentene, which strongly urged us to investigate the influence of cofeed of 1-butene and 1-pentene.

As shown in Table 6, the P/E ratio was 6.3 with only 1-butene as the reactant, catalyzed by Z-1 zeolite, while it was 2.3 when 1-pentene was used as the only reactant. However, when both 1-butene and 1-pentene were the reactants, the P/E ratio was 3.5, which is between 2.3 and 6.3. This result indicated that the dimerization of C_4^{2-} and C_5^{2-} to C_9^{2-} may not happen in a mixed system; otherwise, the P/E ratio would be higher than 6.3. In order to investigate more distinctly whether interplays exist between the catalytic cracking of 1-butene and 1-pentene in the mixed system, we attempted to do a quantitative analysis directly. First, we supposed that 1 mol of 1-butene (56 g) and 1 mol of 1-pentene (70 g) were individually added to reactors under the same conditions. According to the output distribution in Table 6, the output mass of each substance and the conversion of butenes or pentenes can be found (Table 7, entries 1 and 2). If there were no interplays between the catalytic cracking of 1-butene and that of 1-pentene in the mixed system, the output mass of each substance (Table 7, entry 3) with both reactants in one reactor would be easily calculated, which was just the sum of those in the catalytic cracking of 1-butene (Table 7, entry 1) and 1-pentene (Table 7, entry 2), respectively. Then the supposed conversions of butenes and pentenes could be calculated, which were 22.7% and 75.8%, respectively, in an apparent decrease of both. This is caused by the catalytic cracking of 1-butene to produce pentenes and the catalytic cracking of 1-pentene to produce butenes. Essentially, the actual capacity of conversion did not decrease. However, in our practical experiment, if 56 g of 1-butene and 70 g of 1-pentene were placed in one reactor, the output mass of butenes and pentenes (Table 7, entry 4) were higher than the supposed mass in Table 7, entry 3, with a correspondingly lower actual conversion of butenes and pentenes. According to Le Chatelier's principle, an internal reaction caused by an external disturbance would oppose the initial change.[48] As the catalytic cracking of 1-butene was a reversible reaction and could produce pentenes if external 1-pentene was added, on the basis of Le Chatelier's principle, this external disturbance would inhibit 1-butene conversion. Similarly, adding 1-butene to the reactor in the catalytic cracking of 1-pentene would also suppress its conversion. Therefore, in the mixed system, the conversion of butenes and pentenes both decreased.

For extraction of the butenes and pentenes and normalization of the production distribution, the selectivity of each production in entries 3 and 4 is shown in Table 8. It is interesting to note that the selectivity of each product in entry 3 is similar to the selectivity in entry 4. In addition, the P/E ratios were 3.1 and 3.5, respectively, which are also similar. This phenomenon indicated that the reaction pathways of catalytic cracking of both 1-butene and 1-pentene experienced no change in the mixed system. In conclusion, a cofeed of 1-butene and 1-pentene had no significant influence on the catalytic cracking reaction pathways but had some effects on the conversion of 1-butene and 1-pentene.

3.5. Possible Reaction Mechanism for the Conversion of 1-Pentene. To figure out the reasons weak acid sites favor pathways II′ and II′-2, while pathways I′ and II′-1 require strong acid sites, the possible reaction mechanism for the conversion of 1-pentene was investigated.

The structural isomers of pentene consist of *n*-pentene and isopentene. On one hand, *n*-pentene may form three kinds of pentyl carbenium ions: namely, 1-pentyl carbenium ion, 2-

DOI: 10.1021/cs501967r
ACS Catal. 2015, 5, 4048−4059

pentyl carbenium ion, and 3-pentyl carbenium ion. 1-Pentyl carbenium ion can crack to ethene and 1-propyl carbenium ion through β-scission. Modes of β-scission are classified by the types of involved carbenium ions: A (tertiary−tertiary), B (secondary−tertiary), C (secondary−secondary), D type (primary−secondary), E (primary−tertiary), and F (primary−primary).[34] Type A is the most energetically favored form of cracking, and type F, which involves only primary carbenium ions, is energetically unfavorable. As 1-pentyl carbenium ion and 1-propyl carbenium ion are primary carbenium ions, this cracking process undergoes type F β-scission. Similarly, through β-scission, 3-pentyl carbenium ion can crack to methyl carbenium ion, which is energetically unstable. On the other hand, four kinds of pentyl carbenium ions, i.e. 2-methyl-1-butyl carbenium ion, 2-methyl-2-butyl carbenium ion, 3-methyl-1-butyl carbenium ion, and 3-methyl-2-butyl carbenium ion, can be converted from isopentene. The cracking of 2-methyl-1-butyl carbenium ion undergoes type F β-scission, and the cracking of 2-methyl-2-butyl carbenium ion and 3-methyl-2-butyl carbenium ion can produce methyl carbenium ion. To sum up, there are only two kinds of pentyl carbenium ions (2-pentyl carbenium ion and 3-methyl-1-butyl carbenium ion) whose cracking processes are energetically favorable.[7−9] The monomolecular cracking of 1-pentene is shown in Scheme 3 (pathway I′).

Scheme 3. Possible Forms of β-Scission of C_5^+ over ZSM-5

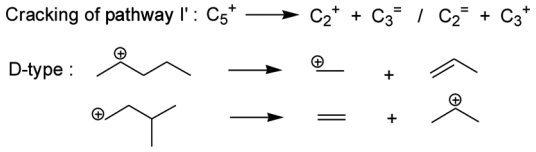

Miyaji and co-workers[7] have investigated the dimerization cracking of 2-methyl-2-butene at the initial stage over SAPO-5, suggesting that first 2,3,4,5-tetramethyl-2-hexyl carbenium ion (X) and 3,4,5-trimethyl-3-heptyl carbenium ion (Y) were preferentially produced by dimerization of 3-methyl-2-butyl carbenium ion with 2-methyl-2-butene at the monosubstituted olefinic carbon and 2-methyl-1-butene at the unsubstituted olefinic carbon, respectively.[7] Isomerization of pentenes was sufficiently faster than the cracking and/or dimerization to maintain an equilibrium.[49] Therefore, although the feedstock in our experiments was 1-pentene, the dimerization reactions were similar to those using 2-methyl-2-butene as feedstock, producing decyl carbenium ions X and Y preferentially. Then X and Y isomerized to other decyl carbenium ions which could crack to butene and hexene though β-scission. As the isomerization which followed the protonated cyclopropane mechanism requires bulky intermediates, X and Y preferentially isomerizes to the decyl carbenium ions with four and three methyls, respectively. There are 11 kinds of structural isomers of decene with four methyls. Correspondingly, 59 kinds of decyl carbenium ions exist theoretically. Among all of the forms, there are 24 kinds of decyl carbenium ions that can crack to either butenes with hexyl carbenium ions or hexenes with butyl carbenium ions. The cracking of 14 kinds of decyl carbenium ions undergo type D, E, or F β-scission, which all involve primary carbenium ions, while only 10 kinds of decyl carbenium ions crack through type A, B, or C β-scission, which involve secondary or tertiary carbenium ions. It has been reported that the reaction rate of type C is 20 times faster than that of type D;[34] therefore, we suppose that X preferentially isomerizes to these 10 kinds of decyl carbenium ions (Scheme S1a in the Supporting Information) whose cracking undergoes type A, B, or C β-scission. The cracking of these 10 kinds of decyl carbenium ions to butenes and hexyl carbenium ions or hexenes and butyl carbenium ions is shown in Scheme 4. In

Scheme 4. Possible Forms of β-Scission of C_{10}^+ (with Four Methyls) over ZSM-5

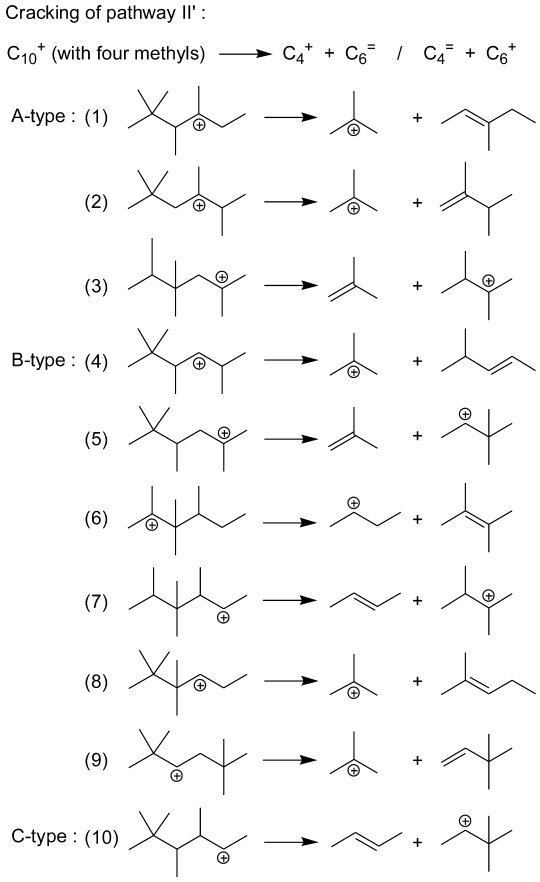

terms of the decene with three methyls, 16 kinds of structural isomers existed, from which 118 kinds of decyl carbenium ions could be produced in theory. Among these, 46 kinds of decyl carbenium ions could crack to butenes with hexyl carbenium ions or hexenes with butyl carbenium ions, only 16 kinds of which could occur through type A, B, or C β-scission (Scheme 5). These 16 kinds of decyl carbenium ions could be formed through isomerization reactions from Y (Scheme S1b in the Supporting Information). In total, there are 26 kinds of decyl carbenium ions that could crack to butene or hexene and were energetically favorable (pathway II′, Schemes 4 and 5). On comparison of Scheme 3 with Schemes 4 and 5, it is obvious that pathway I′ proceeded through a primary cation but pathway II′ mainly proceeded through a secondary or tertiary carbenium ion. This is why the Arrhenius activation energy of the former is higher. Thus, pathway I′ needs strong acid sites to reduce the relatively high activation energy. This mechanism could reasonably explain the phenomena that pathway I′ was promoted (a value decreased) when the HC/LC ratio was improved.

The hexenes produced from pathway II′ could continue to crack, and its structural isomers consist of one linear hexene,

DOI: 10.1021/cs501967r
ACS Catal. 2015, 5, 4048−4059

Scheme 5. Possible Forms of β-Scission of C_{10}^+ (with Three Methyls) over ZSM-5

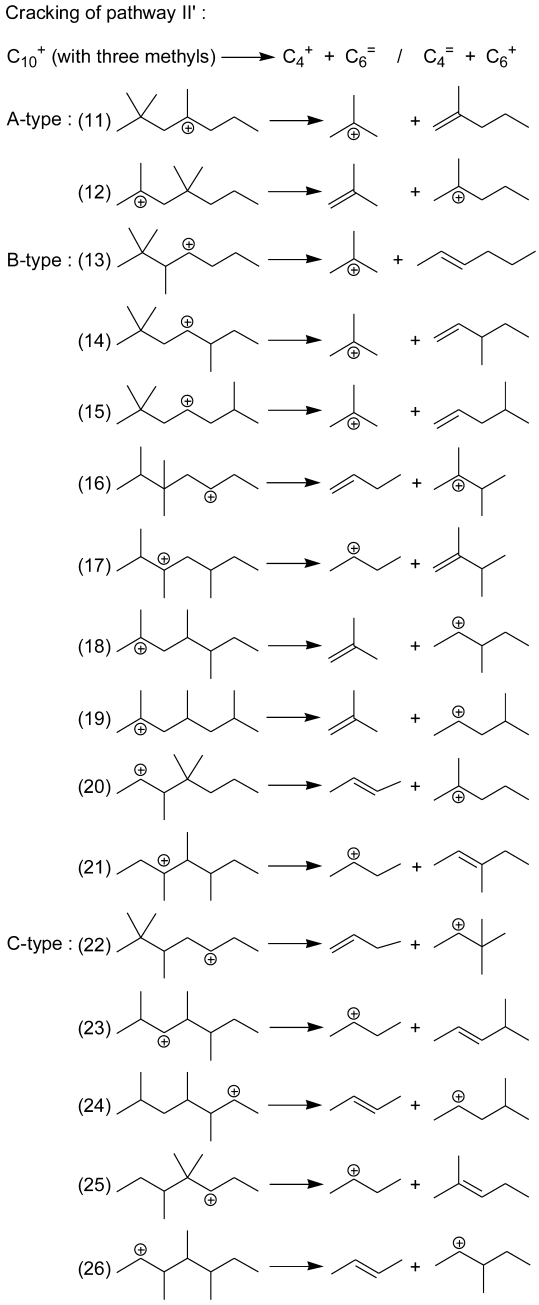

two methylpentenes, and two dimethylbutenes. Thus, 17 kinds of hexyl carbenium ions exist theoretically, among which there are 9 kinds of hexyl carbenium ions cracking through type F β-scission or producing methyl carbenium ions. Among the remaining 8 kinds of hexyl carbenium ions, 4-methyl-2-pentyl carbenium ion, 2-hexyl carbenium ions, and 2,3-dimethyl-1-butyl carbenium ions could crack to propene. The cracking of the first undergoes type C β-scission,[34] and the cracking of the last two undergoes type D β-scission. As mentioned above, the reaction rate of type C is 20 times faster than that of type D.[34] Hence, pathway II′-2 mainly undergoes type C β-scission (Scheme 6). All 5 kinds of hexyl carbenium ions that could crack to ethene or butene undergo type D or E β-scission[34] (Scheme 6, pathway II′-1). Apparently, pathway II′-1 involves primary carbenium ions, but pathway II′-2 proceeds through

Scheme 6. Possible Forms of β-Scission of C_6^+over ZSM-5

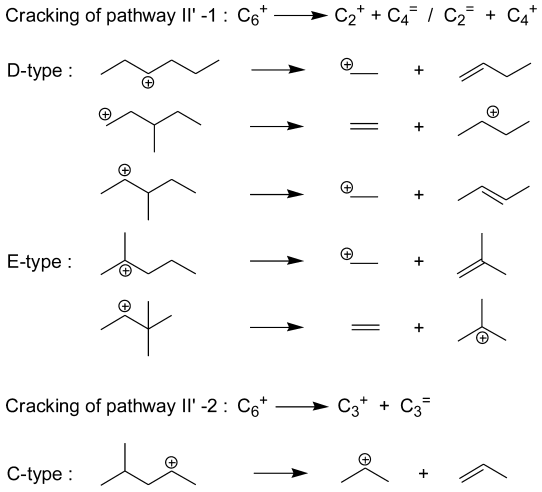

secondary carbenium ion. Therefore, pathway II′-1 needed strong acid sites, while weak acid sites preferred pathway II′-2. The phenomenon that pathway II′-1 was promoted (b value decreased) when the HC/LC ratio was improved could be accounted for by this mechanism.

3.6. Coupled Technological Route of C_4^{2-}/C_5^{2-} Catalytic Cracking. The work presented here could provide a technological guideline for highly efficient production of propene from C_4^{2-}/C_5^{2-}. Since in the cofeed system the selectivity of propene and the P/E ratio were not improved while the conversion of butenes and pentenes decreased, the catalytic cracking of 1-butene and of 1-pentene should thus be separated and coupled in order to improve the efficiency of low-value C_4 and C_5 olefins.

It has been clearly revealed that the acid strength of zeolites and reaction temperature influence the main reaction pathways. Therefore, in order to maximize propene, we should choose the optimized reaction conditions for the system of 1-butene (step 1) and 1-pentene conversion (step 2). First, with regard to the acid strength, the results in both previous and present cases have showed that Z-1 with the fewest amount of strong acid sites was the best zeolite for producing propene in the catalytic cracking of 1-butene[31] or 1-pentene (Table 5). Definitely, we chose Z-1 as the catalyst for steps 1 and 2. Second, over Z-1, the effect of reaction temperature on the catalytic cracking of 1-butene and 1-pentene is shown in Tables S3 and S4 in the Supporting Information, respectively. Table S3 shows that with an increase in temperature, the selectivity of propene remained around 60%, and the selectivity of ethene experienced an increase, which led to a decrease in the P/E ratio. Meanwhile, a noteworthy downward trend was observed for the conversion of butenes. Therefore, a suitable reaction temperature for step 1 was 450 °C. In addition, as shown in Table S4, the P/E ratio also decreased with an increase in temperature, but the selectivity of propene reached the highest point at 450 °C. Hence, 450 °C was also the optimized temperature for step 2. Consequently, for the high production of propene, we shall choose the same reaction conditions (catalyst, Z-1; temperature, 450 °C) for steps 1 and 2.

After the investigation of separate experiments for both step 1 and step 2 over Z-1 at 450 °C (Table 9), the process that introduces pentenes, which are the products of step 1, to be the reactant of step 2 while guiding the butenes produced in step 2 to be the reactant of step 1 was simulated. Finally, considering

DOI: 10.1021/cs501967r
ACS Catal. 2015, 5, 4048−4059

Table 9. Reaction Results of Cracking of 1-Butene (Step 1) and Cracking of 1-Pentene (Step 2) over Z-1 at 450 °C

		sel (wt %)					
step	conv(C_4^{2-} or C_5^{2-}) (wt %)	C_2^{2-}	C_3^{2-}	C_4^{2-}	C_5^{2-}	C_6^{2-}	C^0 + H_2 + arom
1[a]	64.7	6.1	51.5		21.0	11.0	10.4
2[b]	85.2	7.0	35.8	35.7		9.7	11.8

[a]Reaction conditions: cat., Z-1, 1.0 g; temperature, 450 °C; pressure, 0.1 MPa; 1-butene flow rate, 40 mL min^{-1}; N_2 flow rate, 320 mL min^{-1}; WHSV, 6.0 h^{-1}; TOS, 1.5 h. [b]Reaction conditions: cat., Z-1, 1.0 g; temperature, 450 °C; pressure, 0.1 MPa; 1-pentene flow rate, 0.2 mL min^{-1}; N_2 flow rate, 320 mL min^{-1}; WHSV, 7.68 h^{-1}; TOS, 0.5 h.

Scheme 7. Coupled Process of 1-Butene Cracking and 1-Pentene Cracking To Produce Propene

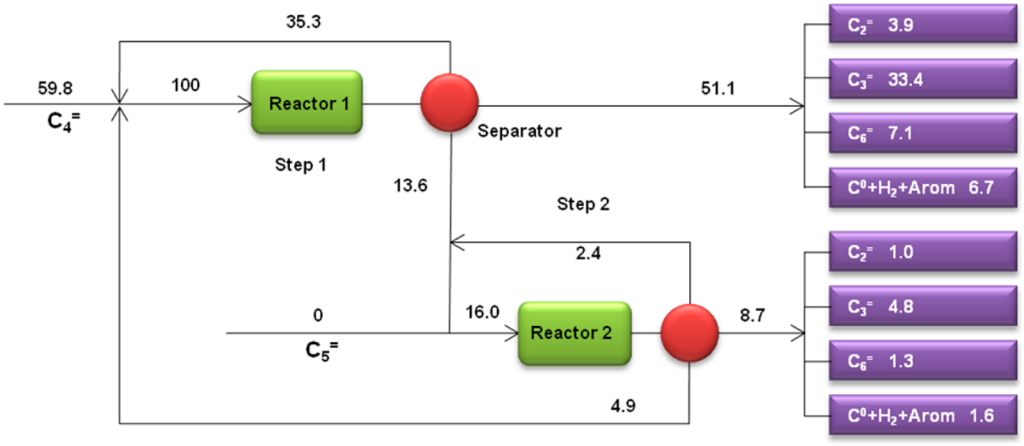

Table 10. Simulation Results of Coupled Process of 1-Butene Cracking and 1-Pentene Cracking

	conditions[a]		sel (wt %)					
route	step 1	step 2	C_2^{2-}	C_3^{2-}	C_6^{2-}	C^0 + H_2 + arom	C_2^{2-} + C_3^{2-}	P/E (wt)
1	59.8, Z-1, 450	0, Z-1, 450	8.2	63.9	14.0	13.9	72.1	7.9
2	75.2, Z-3, 500	0, Z-3, 500	18.1	55.1	7.2	19.6	73.2	3.0
3	0, Z-3, 500	93.3, Z-3, 500	22.1	47.6	9.1	21.2	69.7	2.2
4	0, Z-5, 550	98.0, Z-5, 550	31.6	37.0	1.3	30.1	68.6	1.2

[a]Parameters in the following order: conv(C_4^{2-} or C_5^{2-}) (wt %), zeolite, T (°C).

Table 11. Reaction Results of Cracking of 1-Butene (Step 1) and Cracking of 1-Pentene (Step 2) over Z-5 at 550 °C

		sel (wt %)					
step	conv(C_4^{2-} or C_5^{2-}) (wt %)	C_2^{2-}	C_3^{2-}	C_4^{2-}	C_5^{2-}	C_6^{2-}	C^0 + H_2 + arom
1[a]	85.2	24.6	42.4		2.9	3.0	27.1
2[b]	98.3	28.6	31.9	11.7		0.9	26.9

[a]Reaction conditions: cat., Z-5, 1.0 g; temperature, 550 °C; pressure, 0.1 MPa; 1-butene flow rate, 40 mL min^{-1}; N_2 flow rate, 320 mL min^{-1}; WHSV, 6.0 h^{-1}; TOS, 1.5 h. [b]Reaction conditions: cat., Z-5, 1.0 g; temperature, 550 °C; pressure, 0.1 MPa; 1-pentene flow rate, 0.2 mL min^{-1}; N_2 flow rate, 320 mL min^{-1}; WHSV, 7.68 h^{-1}; TOS, 0.5 h.

the effect of these two extra feedings, the reaction results of a coupled technological route were calculated on the basis of separate experiment data with the detailed calculation process illustrated in Scheme 7. When the feeding mass of 1-butene was supposed to be 100 g, there was 35.3 g of butenes unreacted after the reaction in reactor 1, which would be reused in reactor 1 after separation. Meanwhile, 13.6 g of pentenes was produced for further reaction in reactor 2 and 51.1 g of other products were obtained. In reactor 2, no external pentenes were fed in. Then it was calculated that 16.0 g of pentenes entered reactor 2 and 2.4 g of pentenes underwent backflow. In addition to 8.7 g of products, 4.9 g of butenes was output, which was introduced back to reactor 1 for further utilization. Finally, we needed to introduce 59.8 g of external butenes to this coupled system. In conclusion, the performance of route 1 after a combination of products from steps 1 and 2 is shown in Table 10. The selectivity of propene was 63.9%, and P/E ratio (wt) reached as high as 7.9.

In route 1, the external pentenes were not fed in, because it would lead to a decrease in the P/E ratio. On comparison of the catalytic cracking performance of 1-butene with that of 1-pentene (Table S5 in the Supporting Information), it was found that, under the same conditions, the P/E ratio of the former was higher than that of the latter. This was because part of the pentenes underwent monomolecular cracking which would lead to a P/E ratio of 1, but all butenes underwent dimerization−cracking which led to a higher P/E ratio. Thus, no external pentenes should be fed in route 1 in order to achieve the highest P/E ratio.

DOI: 10.1021/cs501967r
ACS Catal. 2015, 5, 4048−4059

Scheme 8. Coupled Process of 1-Butene Cracking and 1-Pentene Cracking To Produce Ethene

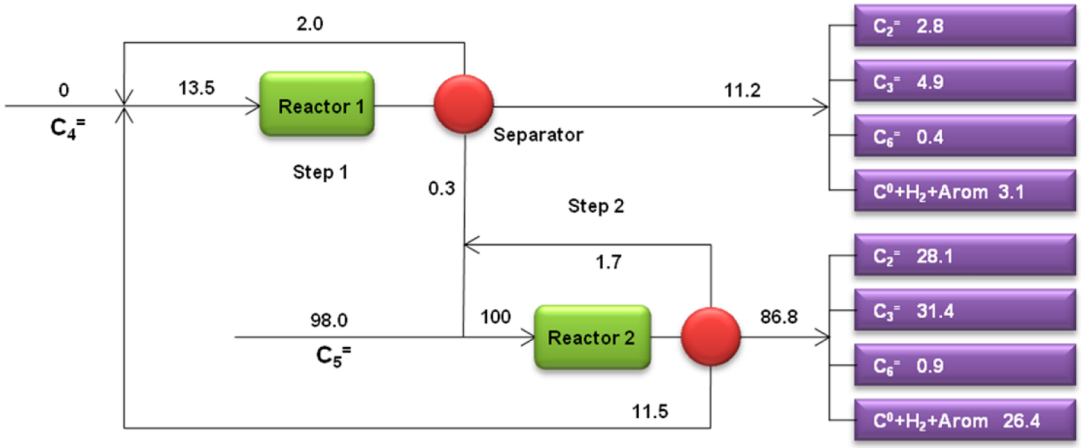

For designing a coupled technological route for producing ethene (route 4), pentenes should be chosen as a feedstock, while external butenes should not. Obviously, Z-5 with the largest amount of strong acid sites was the best zeolite for producing ethene from catalytic cracking of 1-butene[31] or 1-pentene (Table 5). In addition, a high reaction temperature was beneficial to producing ethene (Tables S6 and S7 in the Supporting Information). As a result, the same reaction conditions (catalyst, Z-5; temperature, 550 °C) for steps 1 and 2 should be chosen for the high production of ethene. According to the separated experimental data of steps 1 and 2 over Z-5 at 550 °C (Table 11), we simulated the coupled process of route 4 (Scheme 8), and the results are shown in Table 10. The selectivity of ethene was 31.6%, and the P/E ratio (wt) reached the lowest point at 1.2.

Coupled technological routes with P/E ratios varying between 1.2 and 7.9 could be realized through choosing a suitable feedstock, designing a zeolite with suitable acid strength, and adjusting the reaction temperature. As shown in Table 10, feeding in 1-butene in route 2 performed over Z-3 at 500 °C gave a P/E ratio of 3.0. However, when accounting for 1-pentene, the P/E ratio decreased to 2.2 under the same reaction conditions (route 3). From route 1 to route 4, the selectivity of propene decreased, and the P/E ratio underwent a sharp decline, but the total selectivity of ethene and propene remained at around 70%. At present, the best performance in a single reactor was achieved by using P-modified ZSM-5.[22] The total selectivity of ethene and propene was 74.4%, and the P/E ratio was 3.4. However, in the coupled technological route 1, the P/E ratio reached 7.9; meanwhile, the total selectivity of ethene and propene remained at 72.1%. Thus, this coupled system could provide advantages lying not only in the utilization efficiency of low-value C_4 and C_5 olefins but also in the P/E ratio.

4. CONCLUSIONS

In this paper, we have systematically investigated the catalytic cracking of 1-pentene over ZSM-5. Although the essence of this reaction that the reaction pathways could be controlled by acid strength of catalyst through influencing the activation energy of reaction is the same as that of the catalytic cracking of 1-butene, the specific reaction pathways of catalytic cracking of 1-pentene which contain monomolecular cracking and dimerization–cracking pathways are quite different from the catalytic cracking of 1-butene, which leads to different results. The main reaction pathways of catalytic cracking of 1-pentene were directly controlled by the reaction temperature and acid strength of ZSM-5 zeolite. High reaction temperature benefited pathway I′, while pathway II′ could be promoted at low reaction temperature. Thus, the P/E ratio could be improved through a decrease in the reaction temperature. When the reaction temperature was decreased to 450 °C, pathway II′ become dominant (a = 0.688). Moreover, reaction pathways could be significantly influenced by the acid strength of ZSM-5 zeolite. Strong acid sites would promote the reaction pathways that produced ethene (pathways I′ and II′-1), while weak acid sites preferred the reaction pathways that formed propene (pathways II′ and II′-2). When the HC/LC ratio decreased to 0.244 (Z-1), cracking of 1-pentene mainly took place by pathway II′ (a = 0.904), with b also reaching 0.731 at the same time. Therefore, it would be a wise choice to use a zeolite with a small number of strong acid sites in order to get a high selectivity of propene. In addition, the work presented here provides a guideline for designing a coupled technological route that could produce propene and ethene with various P/E ratios. Also, the P/E ratio (wt) could be controlled between 1.2 and 7.9, with the total mass selectivity of propene and ethene remaining at around 70% at the same time through adjusting the feedstock, reaction temperature, and acid strength of zeolite. As the structure of pentene or butene isomers has no influence on product distributions when they are the reactants, although in our experiment the feedstock was pure 1-pentene or 1-butene, the achievement would still provide extensive applications in industry. It could be anticipated that the technological process which couples the two systems of butene and pentene conversion would be a promising solution for cracking low-value C_4 and C_5 olefins to propene with high utilization efficiency.

■ ASSOCIATED CONTENT

Supporting Information

The Supporting Information is available free of charge on the ACS Publications website at DOI: 10.1021/cs501967r.

Conservation of mass and carbon atoms, reaction scheme of decyl carbenium ion isomerization, and reaction results (PDF)

DOI: 10.1021/cs501967r
ACS Catal. 2015, 5, 4048–4059

AUTHOR INFORMATION

Corresponding Author

*Y.M.L.: tel, +86-21-6223-2058; fax, +86-21-6223-2058; e-mail, ymliu@chem.ecnu.edu.cn.

Notes

The authors declare no competing financial interest.

ACKNOWLEDGMENTS

We gratefully acknowledge the National Key Technology R&D Program (2012BAE05B02), the National Natural Science Foundation Of China (U1462106), the Science and Technology Commission of Shanghai Municipality (12JC1403600), and the Shanghai Leading Academic Discipline Project (B409).

REFERENCES

(1) Koyama, T.; Hayashi, Y.; Horie, H.; Kawauchi, S.; Matsumoto, A.; Iwase, Y.; Sakamoto, Y.; Miyaji, A.; Motokura, K.; Baba, T. *Phys. Chem. Chem. Phys.* **2010**, *12*, 2541−2554.
(2) Wang, B.; Gao, Q.; Gao, J. D.; Ji, D.; Wang, X. L.; Suo, J. S. *Appl. Catal., A* **2004**, *274*, 167−172.
(3) Zhao, G. L.; Teng, J. W.; Zhang, Y. H.; Xie, Z. K.; Yue, Y. H.; Chen, Q. L.; Tang, Y. *Appl. Catal., A* **2006**, *299*, 167−174.
(4) Zhu, X. X.; Liu, S. L.; Song, Y. Q.; Xu, L. Y. *Catal. Lett.* **2005**, *103*, 201−210.
(5) Lu, Y.; He, M. Y.; Shu, X. T.; Zong, B. N. *Appl. Catal., A* **2003**, *255*, 345−347.
(6) Zhu, X. X.; Liu, S. L.; Song, Y. Q.; Xu, L. Y. *Appl. Catal., A* **2005**, *288*, 134−142.
(7) Miyaji, A.; Sakamoto, Y.; Iwase, Y.; Yashima, T.; Koide, R.; Motokura, K.; Baba, T. *J. Catal.* **2013**, *302*, 101−114.
(8) Jeffrey, H. P.; Redondo, A.; Guo, Y. J. *Catal. Today* **1999**, *50*, 517−523.
(9) Bortnovsky, O.; Sazama, P.; Wichterlova, B. *Appl. Catal., A* **2005**, *287*, 203−213.
(10) Gao, X.; Tang, Z.; Zhang, H.; Ji, D.; Lu, G.; Wang, Z.; Tan, Z. *J. Mol. Catal. A: Chem.* **2010**, *325*, 36−39.
(11) Erichsen, M. W.; Svelle, S.; Olsbye, U. *J. Catal.* **2013**, *298*, 94−101.
(12) Choudhary, V. R.; Banerjee, S.; Panjala, D. *J. Catal.* **2002**, *205*, 398−403.
(13) Choudhary, V. R.; Banerjee, S.; Panjala, D. *Microporous Mesoporous Mater.* **2002**, *51*, 203−210.
(14) Smiešková, A.; Rojasová, E.; Hudec, P.; Šabo, L. *React. Kinet. Catal. Lett.* **2004**, *2*, 227−234.
(15) Chen, M.; Yang, Y. *J. Mol. Catal. (China)* **1996**, *10*, 418−422.
(16) Sazama, P.; Dědeček, J.; Gábová, V.; Wichterlová, B.; Spoto, G.; Bordiga, S. *J. Catal.* **2008**, *254*, 180−189.
(17) Quintana-Solórzano, R.; Thybaut, J. W.; Marin, G. B.; Lødeng, R.; Holmen, A. *Catal. Today* **2005**, *107−108*, 619−629.
(18) Guisnet, M.; Magnoux, P. *Appl. Catal., A* **2001**, *212*, 83−96.
(19) Yan, L.; Fu, J.; He, M. Y. *Acta. Petrol. Sinica* **2000**, *16*, 15−26.
(20) Guisnet, M.; Magnoux, P. *Catal. Today* **1997**, *36*, 477−483.
(21) Zhao, G. L.; Teng, J. W.; Xie, Z. K.; Jin, W. Q.; Yang, W. M.; Chen, Q. L.; Tang, Y. *J. Catal.* **2007**, *248*, 29−37.
(22) Xue, N. H.; Chen, X. K.; Nie, L.; Guo, X. F.; Ding, W. P.; Chen, Y.; Gu, M.; Xie, Z. K. *J. Catal.* **2007**, *248*, 20−28.
(23) Zhao, G.; Teng, J.; Jin, W.; Yang, W.; Xie, Z.; Chen, Q. *Chin. J. Catal.* **2004**, *25*, 3−4.
(24) Wang, Z. W.; Jiang, G. Y.; Zhao, Z.; Feng, X.; Duan, A. J.; Liu, J.; Xu, C. M.; Gao, J. S. *Energy Fuels* **2010**, *24*, 758−763.
(25) Jiang, G. Y.; Zhang, L.; Zhao, Z.; Zhou, X. Y.; Duan, A. J.; Xu, C. M.; Gao, J. S. *Appl. Catal., A* **2008**, *340*, 176−182.
(26) Xue, N. H.; Nie, L.; Fang, D. M.; Guo, X. F.; Shen, J. Y.; Ding, W. P.; Chen, Y. *Appl. Catal., A* **2009**, *352*, 87−94.
(27) Xu, R. F.; Liu, J. X.; Liang, C. C.; Jia, W. G.; Li, F. F.; Guo, H. C. *J. Fuel. Chem. Technol.* **2011**, *39*, 449−454.
(28) Epelde, E.; Gayubo, A. G.; Olazar, M.; Bilbao, J.; Aguayo, A. T. *Ind. Eng. Chem. Res.* **2014**, *53*, 4614−4622.
(29) Epelde, E.; Gayubo, A. G.; Olazar, M.; Bilbao, J.; Aguayo, A. T. *Chem. Eng. J.* **2014**, *251*, 80−91.
(30) Wakui, K.; Satoh, K.; Sawada, G.; Shiozawa, K.; Matano, K.; Suzuki, K.; Hayakawa, T.; Yoshimura, Y.; Murata, K.; Mizukami, F. *Catal. Lett.* **2002**, *84*, 259−264.
(31) Lin, L. F.; Qiu, C. F.; Zhuo, Z. X.; Zhang, D. W.; Zhao, S. F.; Wu, H. H.; Liu, Y. M.; He, M. Y. *J. Catal.* **2014**, *309*, 136−145.
(32) Föttinger, K.; Kinger, G.; Vinek, H. *Appl. Catal., A* **2003**, *249*, 205−212.
(33) Sun, Y. X.; Yang, J.; Zhao, L. F.; Dai, J. X.; Sun, H. *J. Phys. Chem. C* **2010**, *114*, 5975−5984.
(34) Buchanan, J. S.; Santiesteban, J. G.; Haag, W. O. *J. Catal.* **1996**, *158*, 279−287.
(35) Guo, Y. H.; Pu, M.; Chen, B. H.; Cao, F. *Appl. Catal., A* **2013**, *455*, 65−70.
(36) Nawaz, Z.; Tang, X. P.; Zhu, J.; Wei, F.; Naveed, S. *Chin. J. Catal.* **2009**, *30*, 1049−1057.
(37) Blasco, T.; Corma, A.; Martinez-triguero, J. *J. Catal.* **2006**, *237*, 267−277.
(38) Moreno, S.; Poncelet, G. *Microporous Mater.* **1997**, *12*, 197−222.
(39) Olson, D. H.; Kokotailo, G. T.; Lawton, S. L.; Meier, W. M. *J. Phys. Chem.* **1981**, *85*, 2238−2243.
(40) Kramer, G. J.; van Santen, R. A.; Emeis, C. A.; Nowak, A. K. *Nature* **1993**, *363*, 529−531.
(41) Rigby, A. M.; Kramer, G. J.; van Santen, R. A.; Aguayo, A. T. *J. Am. Chem. Soc.* **1995**, *117*, 1766−1776.
(42) Post, J. G.; van Hooff, J. H. C. *Zeolites* **1984**, *4*, 9−14.
(43) Corma, A.; Orchillés, A. V. *Microporous Mesoporous Mater.* **2000**, *35*, 21−30.
(44) Emeis, C. A. *J. Catal.* **1993**, *141*, 347−354.
(45) Barzetti, T.; Selli, E.; Moscotti, D.; Forni, L. *J. Chem. Soc., Faraday Trans.* **1996**, *92*, 1401−1407.
(46) Rigby, A. M.; Kramer, G. J.; van Santen, R. A. *J. Catal.* **1997**, *170*, 1−10.
(47) Arrhenius, S. *Z. Phys. Chem.* **1889**, *4*, 226−248.
(48) Liu, Z.; Gren, J.; Hillert, M. *Fluid Phase Equilib.* **1996**, *121*, 167−177.
(49) Maurer, T.; Kraushaar-Czarnetzki, B. *J. Catal.* **1999**, *187*, 202−208.

DOI: 10.1021/cs501967r
ACS Catal. 2015, 5, 4048−4059